24th COBEM - 2017

24th ABCM International Congress of Mechanical Engineering
December 3-8, 2017, Curitiba, PR, Brazil

COBEM-2017-1971
PROCEDURE FOR FLOW REGIME IDENTIFICATION OF DISPERSED BUBBLES IN A GAS-LIQUID MIXTURE FLOWING IN VERTICAL PIPES

Guilherme Marodin Assis
Luiz Eduardo Melo Lima
Federal University of Technology – Paraná, Academic Department of Mechanics
Monteiro Lobato Avenue, km 4, Jardim Carvalho, 84016-210, Ponta Grossa, Paraná, Brazil
guilhermema57@gmail.com, lelima@utfpr.edu.br

Abstract. *Gas-liquid flows are encountered in many industrial applications such as in petroleum industry, where a gas-oil mixture is transported through pipes from the well to the separation and processing facilities. The dispersed flow is one of several gas-liquid flow patterns frequently found in this industrial application. Depending on the dispersed flow regime (viscous, distorted or turbulent), the flow characteristics change significantly, influencing the gas velocity and, therefore, changing the gas fraction along the pipe cross-sections. The goal of this work is to propose a solution procedure for flow regime identification and consequently obtain the main characteristics of the dispersed flow. The solution procedure was implemented in a computational code written in Fortran 95 programming language. For results analysis, it was developed a computational code using Gnuplot tool commands to generate a flow patterns map, which was used to verify the occurrence of the dispersed flow regimes. This analysis considered different work fluids as well as different pipe diameters. The results analysis showed that the solution procedure captures the dispersed flow regimes with a satisfactory precision, despite the differences encountered due to the variation of the properties of the fluids and pipe diameter in the analyzed cases.*

Keywords: *two-phase flow, dispersed flow, bubbles mean diameter, flow regime, flow map.*

1. INTRODUCTION

It is possible to observe the gas-liquid flows occurrence in many industrial applications, for example in the petroleum industry, where a gas-oil mixture is transported through pipes from the well to the separation and processing facilities. In this application, dispersed flow is one of several gas-liquid flow patterns usually found. The dispersed flow regime (viscous, distorted or turbulent) changes flow characteristics significantly, influencing the gas velocity and, therefore, changing the gas fraction along the pipe cross-sections, as well as several other related variables, for example, the pressure gradient (Ishii, 1977; Ishii and Hibiki, 2006).

The viscous or spherical regime exhibits bubbles of uniform size. The distorted regime exhibits deformed bubbles of varying sizes. The turbulent or agitated regime exhibits bubbles which, in addition to being deformed and of varying sizes, are agglomerated. The dispersed flow regimes and their transitions are related to dimensionless numbers, such as Weber, Morton and Reynolds. For example, the bubble size is quantified by the Weber number, which results from a balance between the surface tension forces, which define a maximum bubble size, and the inertia forces of the liquid phase, which act to break the bubbles in smaller sizes. The Morton number also quantifies the bubbles sizes and, in addition, allows the characterization of the distortions increase that occurs in the bubble interface. Finally, the Reynolds number relates inertia forces and viscous forces and characterizes the flow as laminar or turbulent, influencing both the breaking and the coalescence of bubbles (Hinze, 1955; Ishii, 1977; Ishii and Hibiki, 2006; Shoham, 2006).

The viscous regime occurs at high liquid flow rates, where the turbulence forces are high enough to disperse the gas phase into small bubbles of approximately uniform size. From a balance between forces of surface tension and turbulence, Hinze (1955) discovered a characteristic (or maximum) diameter of the dispersed phase for this regime to be stable. Ishii (1977) demonstrated that the drag coefficient for the viscous regime is dependent on the mixture Reynolds number since the bubbles behave as rigid spheres and tend to impose a forces system on the neighborhood fluid, causing an increase in resistance to movement and as a result an increase in mixture viscosity due to the local resistance caused by the shear resulting from the particles movement in relation to the neighborhood fluid. In addition, they have demonstrated that increasing the mixture viscosity generates an increase in the gas fraction and, consequently, an increase in the collision rates between particles (Ishii and Hibiki, 2006). Barnea *et al.* (1982) and Brodkey (1995) found that if turbulence forces are able to distribute the gas phase in bubbles of smaller diameter than their critical diameter definitions, the viscous regime will prevail and the bubbles take the form of solid spheres with low coalescence rates.

The relative velocity of small distorted bubbles was defined by Harmathy (1960) as being inversely proportional to the pipe diameter, different from the relative velocity of the Taylor bubble (bubble with diameter close to the pipe diameter) which increases with the reduction of the pipe diameter (Dumitrescu, 1943; Nicklin, 1962; Davies and Taylor, 1988; Shoham, 2006). In the intermittent flow, the distorted bubbles regime in the liquid piston can be analyzed by considering the relative velocities of the small bubbles and the Taylor bubble, exhibiting a dependence on the pipe diameter. For larger diameters, where the relative velocity of the Taylor bubble is greater than that of the small bubbles, the Taylor bubble drags these small bubbles around it, not allowing them to coalesce. In contrast, when the relative velocity of the small bubbles is greater than that of the Taylor bubble, they tend to agglutinate in the tail region of the Taylor bubble thus forming the intermittent pattern (Shoham, 2006). Ishii (1977) proposed that in the distorted regime, where occurs the formation of turbulent vortices behind a particle, such that the particles behind it exhibit greater resistance to flow, the drag coefficient is dependent only on the bubbles mean diameter and properties of the fluids (Ishii and Hibiki, 2006).

The turbulent regime occurs for gas fractions of approximately 30%. In this condition, the bubbles tend to have a chaotic movement and collide randomly, agglutinating and forming a bubbles cluster. This bubbles cluster behaves similarly to Taylor bubbles but does not occupy the entire pipe section. As long as the dominant forces do not allow the formation of the Taylor bubbles, the turbulent regime will prevail (Shoham, 2006). In the turbulent regime, when a particle suffers an increase in its diameter a wake region is created behind it, allowing the drag of other particles in sequence. Due to the formation of this wake, the smaller bubbles move behind the larger bubbles without an increase in the drag coefficient. However, the increased interaction between the particles, due to the increase in gas concentration, reduces the drag coefficient (Ishii and Hibiki, 2006).

The goal of this work is to propose a procedure for flow regime identification and consequently, obtaining the main characteristics of the dispersed flow. The results obtained by the proposed procedure, for cases of dispersed vertical flow, are evaluated in relation to a classic vertical pattern map, to better visualize the regimes transitions occurrence.

2. MODEL

It is considered a gas-liquid flow in the dispersed pattern flowing in a pipe that has the following characteristics: diameter D, length L, inclination θ (with respect to the plane normal to the gravitational acceleration g), absolute roughness ε, perimeter S, and cross-sectional area A. Figure 1 shows a schematic representation of the dispersed flow and their variables: bubbles mean diameter D_B, cross-sectional area occupied by the liquid A_L, bubbles velocity U_B, liquid velocity U_L, mixture superficial velocity J, liquid fraction ϕ_L, and mixture wall shear stress τ_W (Shoham, 2006).

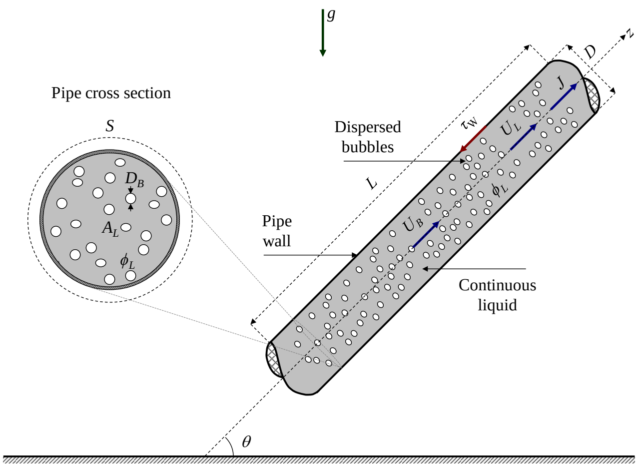

Figure 1. Schematic representation of the dispersed flow and their variables. Adapted from Lima (2011).

2.1 Geometric variables

The maximum value for the dispersed bubbles diameter is called the critical diameter $D_{B,cr}$, which in turn limits the bubbles size so that they do not coalesce to form a Taylor bubble. Bubbles smaller than $D_{B,cr}$ tend to behave as solid spheres. The value of $D_{B,cr}$ is defined by Taitel and Dukler (1976) for horizontal or near-horizontal flows, based on a balance between turbulence and buoyancy forces, as well as Taitel *et al.* (1980) and Barnea *et al.* (1985) for vertical flows, based on a balance between turbulence and surface tension forces, according to Eq. (1) (Shoham, 2006):

$$D_{B,cr} = \begin{cases} 0.375\, D\, C_f\, \mathrm{Fr}^2/\cos\theta & \text{horizontal or near-horizontal} \\ 1.265\, D\, \mathrm{Eo}^{-1/2} & \text{vertical} \end{cases} \tag{1}$$

where $\mathrm{Fr} = J/\sqrt{g\,D(1-\rho_G/\rho_L)}$ is the mixture Froude number, $\mathrm{Eo} = g\,D^2(\rho_L-\rho_G)/\sigma$ is the Eötvös number, ρ_G and ρ_L are the densities of gas and liquid, respectively, σ is the gas-liquid surface tension, and C_f is the turbulent Fanning friction factor defined by Haaland (1983) according to Eq. (2):

$$C_f = \left\{-3.6\,\log\left[\left(\frac{\varepsilon/D}{3.7}\right)^{1.11} + \frac{6.9}{\mathrm{Re}}\right]\right\}^{-2} \tag{2}$$

where $\mathrm{Re} = J\,D/\nu_L$ is the mixture Reynolds number, and $\nu_L \equiv \mu_L/\rho_L$ is the liquid kinematic viscosity.

Calderbank (1958) proposed a definition for a maximum diameter $D_{B,max}$ which allows the bubble stability in the dispersed flow, according to the Eq. (3):

$$D_{B,max} = \left(0.725 + 4.15\,\sqrt{J_G/J}\right)(\sigma/\rho_L)^{3/5}(2\,C_f\,J^3/D)^{-2/5} \tag{3}$$

Depending on their size, bubbles may have different behavior types. For $D_{B,max} \geq D_{B,cr}$ and with relatively high turbulence forces (to cause bubbles to break in sizes smaller than $D_{B,max}$), the bubbles do not agglomerate, hindering coalescence and the dispersed pattern occurrence will prevail. In this case, because of the low collision and coalescence rates, the bubbles are spherical and behave like solid spheres. For $D_{B,max} < D_{B,cr}$ the bubbles tend to deform, and the collision and coalescence rates increase, so the bubbles tend to agglutinate to form a Taylor bubble, resulting in the occurrence of the slug flow pattern (intermittent).

The Sauter mean diameter D_{Sm} is a statistical model that allows a reasonable estimate of the dispersed bubbles mean diameter. It was defined by Sekoguchi *et al.* (1974) and Herringe and Davis (1976), as presented by Kataoka and Serizawa (1990), in such a way that it relates important variables associated with the two-phase flow: the interfacial area concentration a_i and the gas fraction ϕ_G. The interfacial area concentration a_i is the variable governing the mass, momentum, and energy transfers from one fluid to another through the interface. The gas fraction ϕ_G expressed to the phases distribution in the pipe cross-section. The Sauter mean diameter is given by $D_{Sm} = 6\,\phi_G/a_i$. Due to the difficulty of directly determining both the interfacial area concentration a_i as the gas fraction ϕ_G, it is possible to define the Sauter mean diameter D_{Sm}, from semi-empirical correlations, in terms of the primitive flow variables. For example, Eq. (4) proposed by Hibiki *et al.* (2006):

$$D_{Sm} = 1.99\,D\,\mathrm{Eo}^{-0.3325}\,\mathrm{Re}_\epsilon^{-0.239}/\eta \tag{4}$$

where Re_ϵ is a Reynolds number based on kinetic energy dissipation, whose definition is given by Eq. (5):

$$\mathrm{Re}_\epsilon = \left(\epsilon\,D^4/\mathrm{Eo}^2\right)^{1/3}/\nu_L \tag{5}$$

The kinetic energy dissipation ϵ is defined by the sum of the effects contributions resulting from coalescence and break bubbles, as Eq. (6) presented by Hibiki and Ishii (2002):

$$\epsilon = g\,J_G\,e^{-0.0005839\,\mathrm{Re}_L} + \frac{C_f\,J^3}{2\,D}\left(1 - e^{-0.0005839\,\mathrm{Re}_L}\right) \tag{6}$$

where $\mathrm{Re}_L = J_L\,D/\nu_L$ is the liquid Reynolds number.

The dimensionless group η, used to define the Eq. (4) according to the flow phenomenon, is given by Eq. (7):

$$\eta = \begin{cases} 1 & \text{adiabatic flow} \\ 1.22(J_G/J_L)^{-0.17}(\rho_G/\rho_L)^{0.138} & \text{boiling flow} \end{cases} \tag{7}$$

Finally, the bubbles mean diameter, D_B, is considered to be the minimum value between $D_{B,cr}$ and D_{Sm}.

2.2 Kinematic variables

The mixture superficial velocity (the volume center velocity of the mixture) is given by Eq. (8):

$$J = J_G + J_L \tag{8}$$

where $J_G = Q_G/A$ and $J_L = Q_L/A$ are the superficial velocities of gas and liquid, respectively. Q_G and Q_L are the volumetric flow rates of gas and liquid, respectively.

The liquid phase velocity is expressed in terms of the mixture superficial velocity J, the bubbles velocity U_B, and the gas and liquid fractions, ϕ_G and ϕ_L, by Eq. (9):

$$U_L = (J - \phi_G\,U_B)/\phi_L \tag{9}$$

The bubbles velocity U_B is defined by the kinematic model proposed by Nicklin (1962), in which the bubbles move with the mixture superficial velocity J, plus a local drift velocity $V_{\infty,B}$, according to Eq. (10):

$$U_B = C_{0,B}\, J + V_{\infty,B} \tag{10}$$

The distribution parameter $C_{0,B}$ depends on the bubbles mean diameter, according to Eq. (11) (Hibiki and Ishii, 2002):

$$C_{0,B} = \left(1.2 - 0.2\sqrt{\rho_G/\rho_L}\right)\left(1 - e^{-22\, D_B^*}\right) \tag{11}$$

where $D_B^* = D_B/D$ is the dimensionless mean diameter of the dispersed bubbles.

The local drift velocity (the bubbles ascension velocity in a stagnant medium) is given by Eq. (12):

$$V_{\infty,B} = C_{\infty,B}\sqrt{g\, D\,(1-\rho_G/\rho_L)} \tag{12}$$

where $C_{\infty,B}$ is the dimensionless local drift velocity, which in turn is dependent on the dispersed flow regime by Eq. (13):

$$C_{\infty,B} = \begin{cases} \frac{21.6}{D_B^*\sqrt{\mathrm{Ar}}}\left[\frac{(1+\psi)\,\psi^{4/3}\,\phi_L^3}{1+\psi\,\phi_L^{9/7}}\right] & \text{viscous regime} \\ \sqrt{2}\,\mathrm{Eo}^{-1/4}\,\phi_L^{7/4} & \text{distorted regime} \\ \sqrt{2}\,\mathrm{Eo}^{-1/4} & \text{turbulent regime} \end{cases} \tag{13}$$

where $\psi = 0.55\,\{[1 + 0.01\,(D_B^*)^3\,\mathrm{Ar}]^{4/7} - 1\}^{3/4}$ is a dimensionless group and $\mathrm{Ar} = g\, D^3\,(1-\rho_G/\rho_L)/\nu^2$ is the Archimedes number.

2.3 Mixture variables and phases fractions

In dispersed flow, the density ρ and the dynamic viscosity μ of the gas-liquid mixture may be defined in terms of the phases properties, weighted by their respective fractions, according to Eqs. (14) and (15):

$$\rho = \rho_G\,\phi_G + \rho_L\,\phi_L \tag{14}$$

$$\mu = \mu_G\,\phi_G + \mu_L\,\phi_L \tag{15}$$

The gas fraction ϕ_G is defined using the drift kinematic law (Zuber and Findlay, 1965), according to Eq. (16):

$$\phi_G = J_G/U_B \equiv J_G/(C_{0,B}\, J + V_{\infty,B}) \tag{16}$$

Using Eq. (16) together with the saturation condition ($\phi_L = 1 - \phi_G$) it is possible to obtain an implicit function of ϕ_L, since the local drift velocity $V_{\infty,B}$ has a functional dependence on ϕ_L, according to Eq. (17), which can be solved numerically using the secant method (Press *et al.*, 1996):

$$f(\phi_L) = J_G - (1-\phi_L)(C_{0,B}\, J + V_{\infty,B}) = 0 \tag{17}$$

2.4 Regimes transitions

Both the viscous regime and the distorted regime occurs for $\phi_L \geq 0.7$, otherwise, the transition from the dispersed pattern to the intermittent pattern may occur. In addition, the transitions between the viscous, distorted and turbulent regimes are defined in terms of dimensionless numbers: the Morton number, Eq. (18); the Reynolds number based on the local drift velocity, Eq. (19); Weber number based on the bubbles velocity in relation to the superficial mixture velocity, Eq. (20) (Ishii, 1977; Ishii and Hibiki, 2006).

$$\mathrm{Mo} = g\,(1-\rho_G/\rho_L)\,\mu^4/\left(\rho_L\,\sigma^3\right) \tag{18}$$

$$\mathrm{Re}_{\infty,B} = V_{\infty,B}\, D_B/\nu_L \tag{19}$$

$$\mathrm{We}_{\infty,B} = (U_B - J)^2\, D_B\,\rho_L/\sigma \tag{20}$$

In the viscous regime, the particles movement is strongly affected by the viscosity, such that the particles spherical shape is not distorted by the instabilities generated from the turbulence associated with the surrounding fluid movement the particles. The criterion for the transition from the viscous to the distorted regime is based on the Morton number, Mo, and Reynolds number, $\mathrm{Re}_{\infty,B}$, defining whether or not the particle will be distorted by turbulence. The viscous regime occurs for $\mathrm{Mo}^{1/4} < 36\sqrt{2}\,(1 + 0.1\,\mathrm{Re}_{\infty,B}^{3/4})/\mathrm{Re}_{\infty,B}^2$. For $\mathrm{Mo}^{1/4} \geq 36\sqrt{2}\,(1 + 0.1\,\mathrm{Re}_{\infty,B}^{3/4})/\mathrm{Re}_{\infty,B}^2$ the bubbles tend to deform and move more randomly, evidencing the occurrence of the distorted regime. The transition to the turbulent regime is related to the liquid fraction ϕ_L and Weber number $\mathrm{We}_{\infty,B}$. The Weber number is a relation between inertia forces and surface tension forces that allows quantifying the maximum stable size of the bubbles. For the turbulent regime to occur it has to be $0.48 < \phi_L < 0.7$ and $\mathrm{We}_{\infty,B} \leq 8$, above this $\mathrm{We}_{\infty,B}$ value the bubbles tend to coalesce to form a spherical cap (transition to the intermittent pattern) (Ishii, 1977; Ishii and Hibiki, 2006).

3. NUMERICAL PROCEDURE

The numerical procedure developed in this work is based on the dispersed flow regimes (viscous, distorted and turbulent) proposed by Ishii (1977) and Ishii and Hibiki (2006), which can be used to identify the dispersed flow regime in a given condition and, consequently, to determine the dispersed flow variables according to each of these regimes. A flowchart of this numerical procedure for identifying the flow regime is presented in Fig. 2.

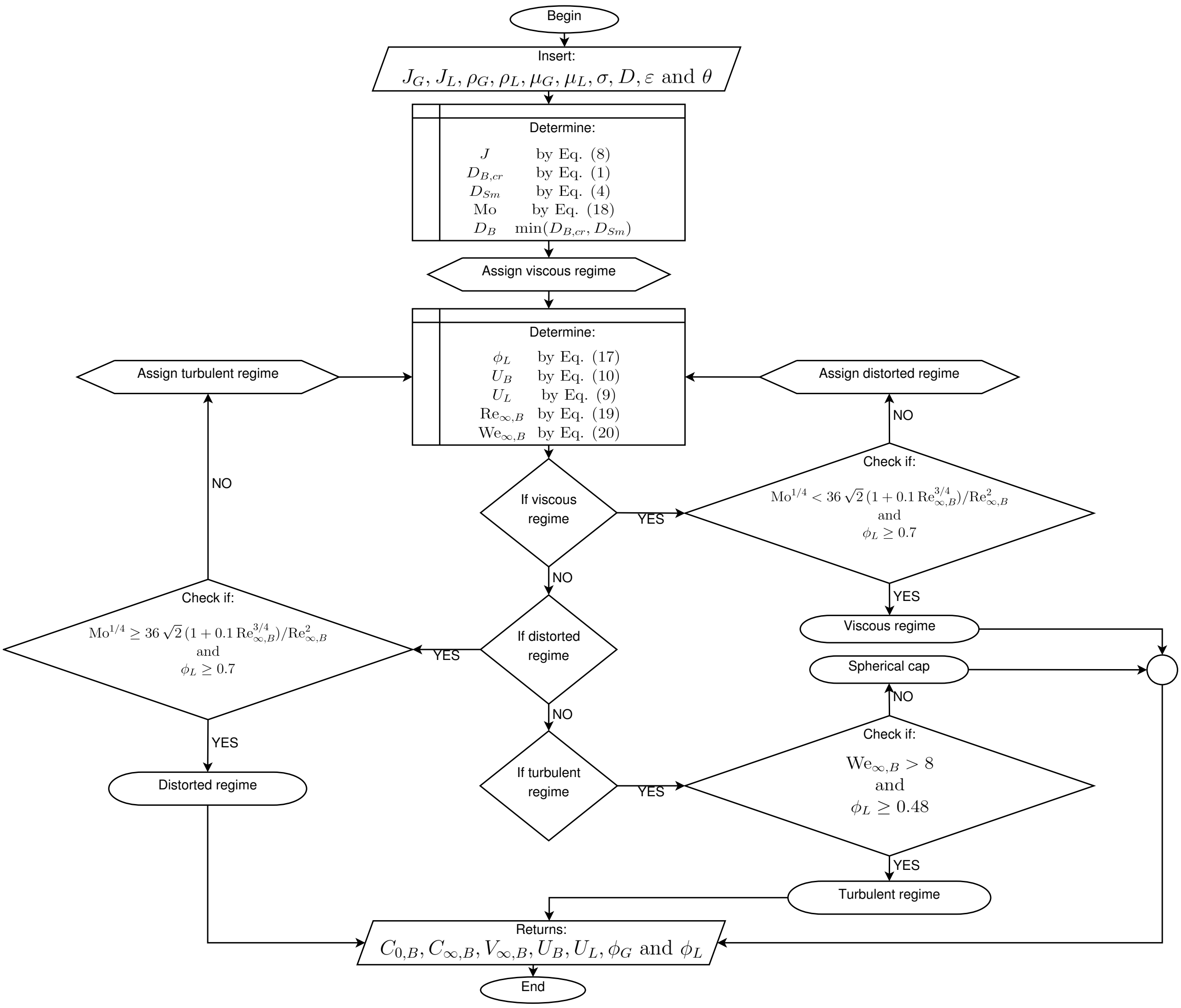

Figure 2. Flowchart of the numerical procedure for identifying the flow regime.

To obtain results with the numerical procedure for identifying the flow regime described by the flowchart presented in Fig. 2, a computational code written in Fortran 95 programming language was developed.

For visualization and analysis of the results, it was developed other computational code using Gnuplot tool commands with the goal to generate a flow patterns map (Taitel *et al.*, 1980), which allows viewing and verifying the occurrence of dispersed bubbles regimes (viscous, distorted and turbulent).

4. RESULTS AND DISCUSSION

In this results analysis, three gas-liquid flow cases in vertical tubes are used, as described by Tab. 1. Case 1 is an air-water flow, case 2 is an air-glycerin flow and case 3 is a gas-oil flow. For these three cases, four different tube diameters were considered (13 mm, 26 mm, 52 mm and 78 mm). The liquid superficial velocity values are considered to vary from 0.01 m/s to 100 m/s. For each liquid superficial velocity value, gas superficial velocity values are considered to vary from 0.01 m/s up to limits established so that there is no transition from the dispersed pattern to other flow patterns.

Table 1. Gas-liquid flow cases analyzed.

Case	P / [Pa]	T / [°C]	Fluids	ρ / [kg/m^3]	μ / [kg/(m.s)]	σ / [N/m]
1	101325	25	Air	1.18	1.8×10^{-5}	–
			Water	997.0	8.9×10^{-4}	0.072
2	101325	25	Air	1.18	1.8×10^{-5}	–
			Glycerin	1257.0	1.5×10^{-3}	0.063
3	101325	15	Natural gas	0.84	1.7×10^{-5}	–
			Oil	850.0	6.0×10^{-3}	0.025

4.1 Case 1: air-water flow

Figure 3 presents the distribution of the dispersed flow regimes for case 1 (air-water) in the vertical pattern map (Taitel *et al.*, 1980), obtained according to the flowchart presented in Fig. 2.

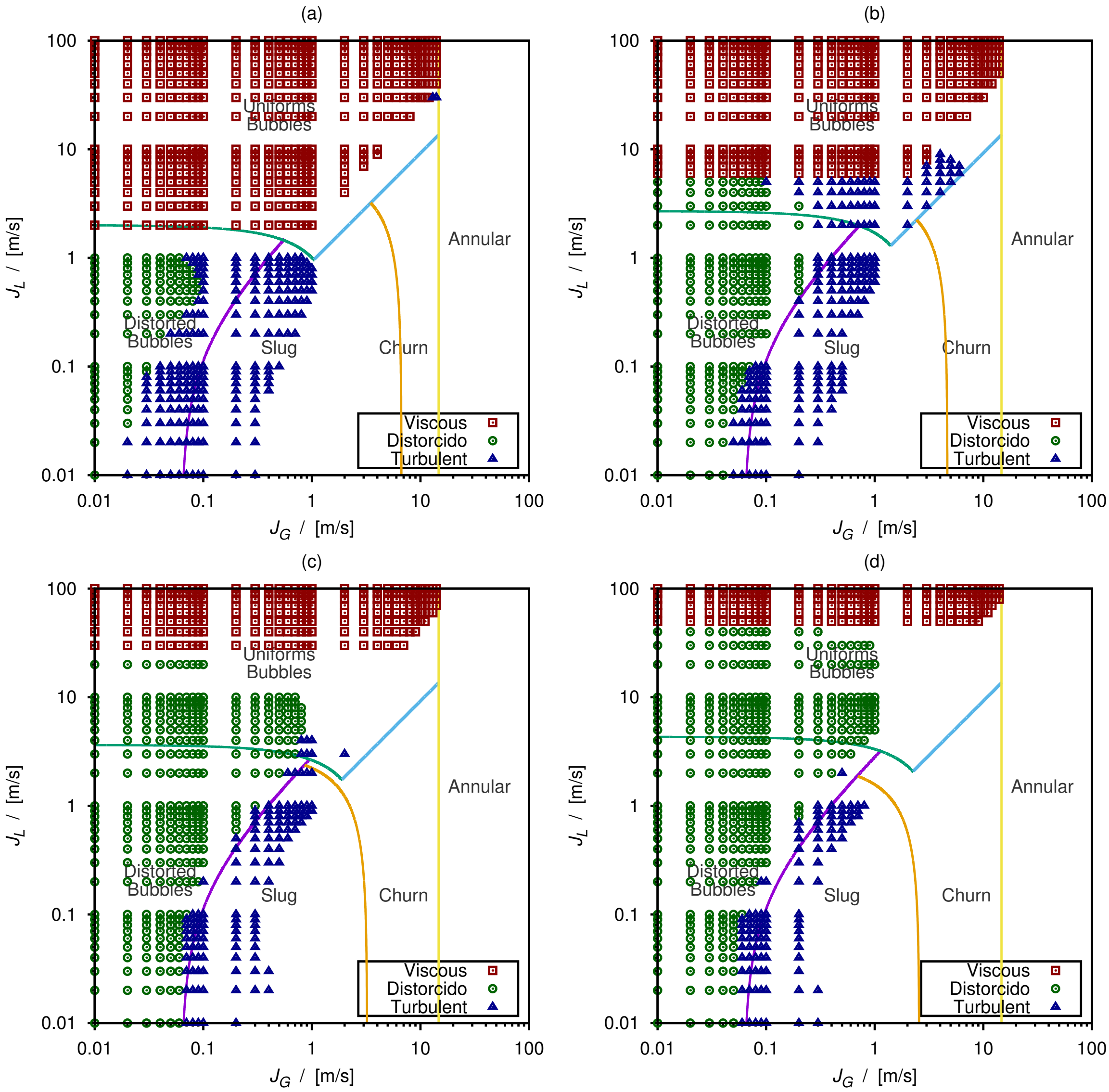

Figure 3. Distribution of dispersed flow regimes in the vertical pattern map for air-water flow in different pipe diameters: (a) 13 mm; (b) 26 mm; (c) 56 mm; (d) 78 mm.

In case 1, for low gas and liquid flow rates, it is possible to observe the occurrence of the distorted and turbulent regimes in the pattern map, since the low liquid superficial velocities do not promote sufficient turbulence forces to maintain the bubble size uniform. When the superficial velocities of gas and liquid are close prevails to the occurrence of the distorted regime. For each value of the low liquid superficial velocities, the increase of the gas superficial velocity results in a chaotic behavior for the bubbles, prevailing to the occurrence of the turbulent regime. For high liquid superficial velocities, the turbulence forces are sufficient to maintain the bubbles of uniform sizes, prevailing to the occurrence of the viscous regime, mainly in low Reynolds numbers.

The pipe diameter increase results in an increase in bubble size because the flow becomes more turbulent (decreasing the viscous regime occurrence), prevailing the distorted regime occurrence even for high liquid superficial velocities. The pipe diameter increase also promotes a decrease in the turbulent regime occurrence, due to the increased turbulence that causes the bubbles to be more distorted, but not to the point where the flow becomes chaotic, as a consequence of the Weber number value remains approximately constant. In addition, the properties of the fluids also influence the distribution of the flow regimes, since the specific masses, the liquid viscosity and the gas-liquid surface tension influence the numbers of Morton, Reynolds and Weber, which in turn define the transitions of regimes. This explains the differences between the distributions of the regimes and the transitions in the pattern map, which becomes more pronounced as the diameter of the tube increases.

4.2 Case 2: air-glycerin flow

Figure 4 presents the distribution of the dispersed flow regimes for case 2 (air-glycerin) in the vertical pattern map (Taitel *et al.*, 1980), obtained according to the flowchart presented in Fig. 2.

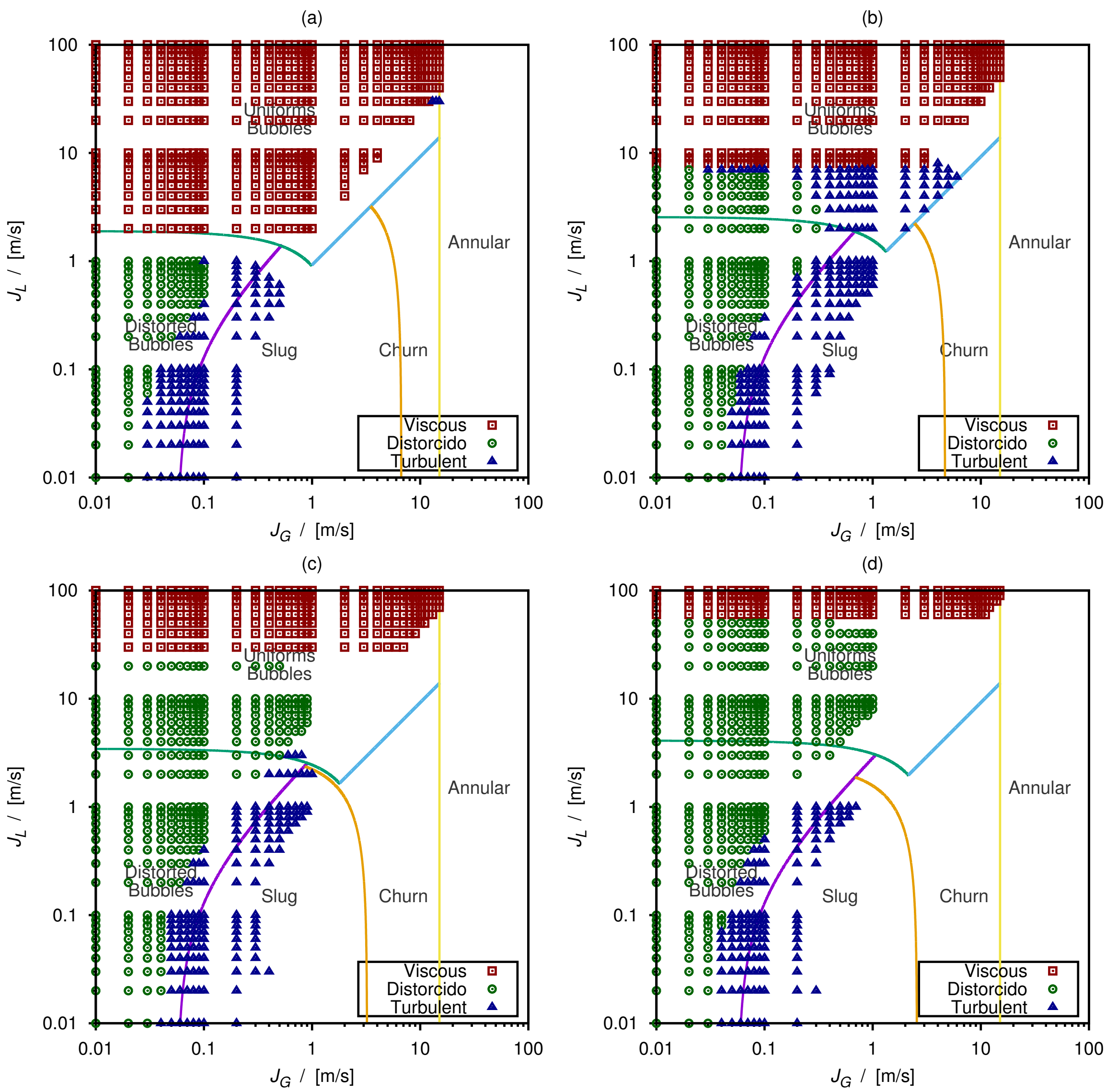

Figure 4. Distribution of the dispersed flow regimes in the vertical pattern map for air-glycerin flow in different pipe diameters: (a) 13 mm; (b) 26 mm; (c) 56 mm; (d) 78 mm.

For case 2, the distribution of dispersed flow regimes in the pattern map shows a behavior similar to that presented in case 1. The differences observed between case 2 and case 1 are due to changes in the properties of the fluids. For example, the glycerin surface tension, being smaller than that of water, results in greater distortions in bubble size. The flow tends to be less turbulent due to the lower values of Reynolds numbers than in the previous case. More due to the large distortions caused by the Morton number (increase in bubble size), the distorted regime tends to prevail more than in case 1. The turbulent regime also occurs at a lower frequency since the inertial forces are not sufficient for the flow to be chaotic, only at transition limits, where the gas superficial velocities are higher than liquid superficial velocities. The effect related to increasing the diameter of the tube in the distribution of the regimes is similar to that in case 1. As a consequence, the distorted regime occurs more frequently.

4.3 Case 3: gas-oil flow

Figure 5 presents the distribution of the dispersed flow regimes for case 2 (gas-oil) in the vertical pattern map (Taitel *et al.*, 1980), obtained according to the flowchart presented in Fig. 2.

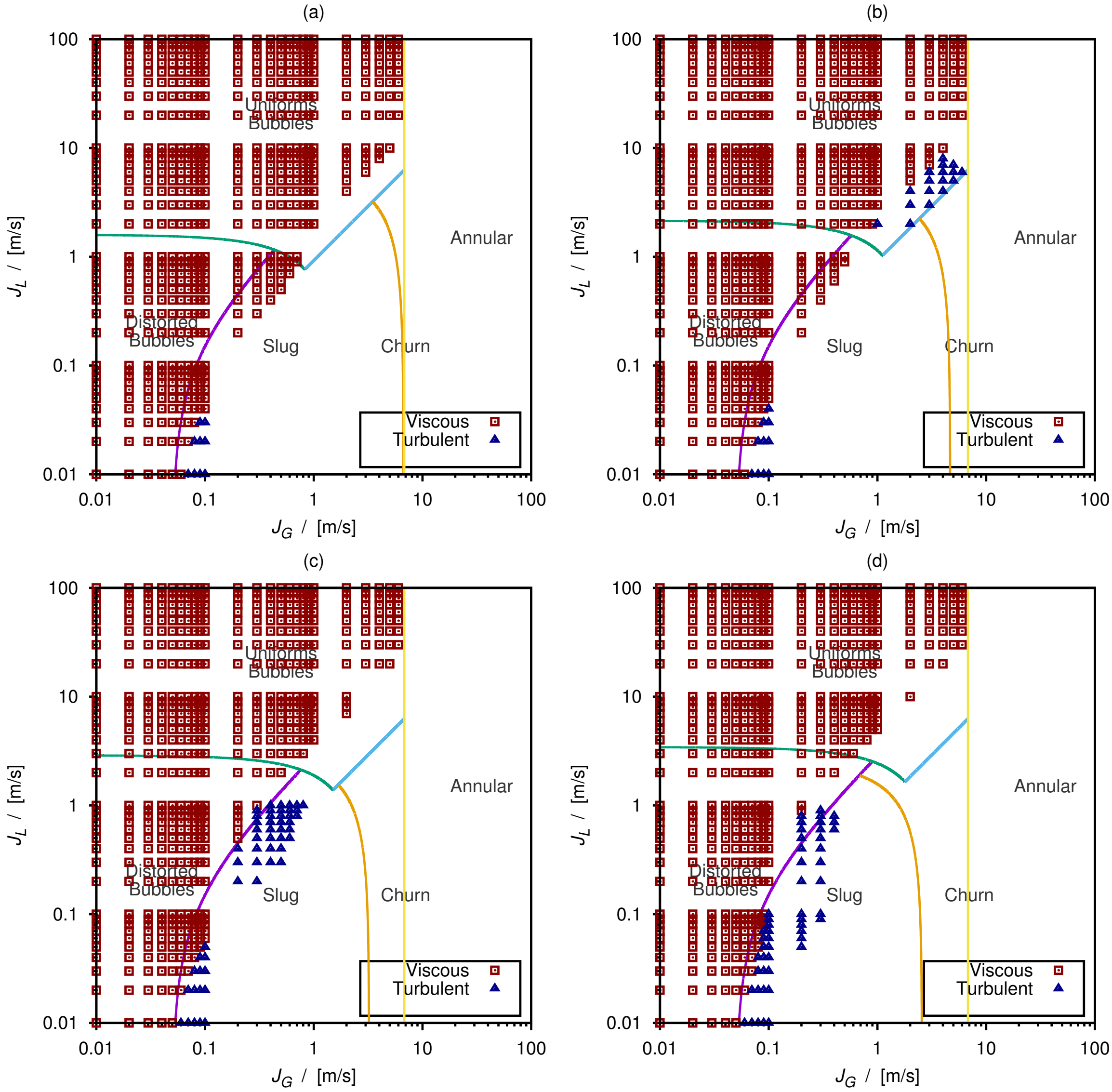

Figure 5. Distribution of dispersed flow regimes in the vertical pattern map for gas-oil flow in different pipe diameters: (a) 13 mm; (b) 26 mm; (c) 56 mm; (d) 78 mm.

In case 3, due to the high viscosity of the liquid and the low relative velocities, the predominant regime is the viscous, presenting the lowest Reynolds number values of the three cases analyzed. As a result, the occurrence of the turbulent regime is difficult, appearing only in the transition to the intermittent pattern. It is not possible to observe the occurrence of the distorted regime in any of the diameters analyzed. Although the surface tension has a great influence on the growth and deformation process of the bubbles, the viscosity of the liquid overlaps the effect of the surface tension such that the bubbles do not have enough energy to grow and remain approximately uniform in size.

5. CONCLUSIONS

In this work, a solution procedure was developed that allows the regime determination for the dispersed flows. With this solution procedure, it is also possible to estimate the dispersed flow variables with a reasonable precision since the equations used are based on the flow phenomenology. The results obtained were verified by comparison against a classical flow patterns map for vertical pipes.

Through the results analysis, it was observed that the change in properties of the fluids, performed through the choice of different working fluids, significantly influences the regimes distribution in the map of vertical flow patterns. For example, for liquids with high viscosity, the flow tends to be laminar, such that the viscous regime occurrence is predominant. Gas-liquid surface tension is another property that also influences the regimes distribution of dispersed flow, causing distortions at the dispersed bubbles interface.

Despite the divergences presented, related to changes in properties of the fluids and diameter, the use of the flow pattern map for results analysis was of great importance in order to visualize and verify the occurrence of dispersed flow regimes. Moreover, the transition criteria adopted for the regimes identification and the transition criteria adopted for the flow pattern map construction are different, although both are mechanistic in nature.

6. ACKNOWLEDGEMENTS

The authors thank the Federal University of Technology – Paraná for the support received for the development of this work and the participation in this event.

7. REFERENCES

Barnea, D., Shoham, O., Taitel, Y. and Dukler, A.E., 1985. "Gas-liquid flow in inclined tubes: flow pattern transitions for upward flow". *Chemical Engineering Science*, Vol. 40, No. 1, pp. 131–136.

Barnea, D., Shoham, O. and Taitel, Y., 1982. "Flow pattern transition for vertical downward two phase flow". *Chemical Engineering Science*, Vol. 37, No. 5, pp. 741–744. ISSN 0009-2509. doi:http://dx.doi.org/10.1016/0009-2509(82)85034-3. URL http://www.sciencedirect.com/science/article/pii/0009250982850343.

Brodkey, R.S., 1995. *The phenomena of fluid motions*. Addison-Wesley series in chemical engineering. Dover Publications. ISBN 9780486686059. URL https://books.google.com.br/books?id=ueD3xhVUAOYC.

Calderbank, P.H., 1958. "Physical rate processes in industrial fermentation. part i: the interfacial area in gas-liquid contacting with mechanical agitation". *Trans. Inst. Chem. Eng.*, Vol. 36, No. 5, pp. 433–440.

Davies, R.M. and Taylor, S.G., 1988. "The mechanics of large bubbles rising through extended liquids and through liquids in tubes". In P. Pelcé, ed., *Dynamics of Curved Fronts*, Academic Press, San Diego, pp. 377–392. ISBN 978-0-12-550355-6. doi:http://dx.doi.org/10.1016/B978-0-08-092523-3.50041-1. URL http://www.sciencedirect.com/science/article/pii/B9780080925233500411.

Dumitrescu, D.T., 1943. "Strömung an einer luftblase im senkrechten rohr". *ZAMM-Journal of Applied Mathematics and Mechanics/Zeitschrift für Angewandte Mathematik und Mechanik*, Vol. 23, No. 3, pp. 139–149.

Haaland, S.E., 1983. "Simple and explicit formulas for the friction factor in turbulent pipe flow". *Journal of Fluids Engineering*, Vol. 105, No. 1, pp. 89–90.

Harmathy, T.Z., 1960. "Velocity of large drops and bubbles in media of infinite or restricted extent". *AIChE Journal*, Vol. 6, No. 2, pp. 281–288.

Herringe, R.A. and Davis, M.R., 1976. "Structural development of gas-liquid mixture flows". *J. Fluid Mech.*, Vol. 73, No. 1, pp. 97–123.

Hibiki, T. and Ishii, M., 2002. "Distribution parameter and drift velocity of drift-flux model in bubbly flow". *International Journal of Heat and Mass Transfer*, Vol. 45, No. 4, pp. 707–721. ISSN 0017-9310. doi:10.1016/S0017-9310(01)00195-8. URL http://www.sciencedirect.com/science/article/B6V3H-44C0R4X-3/2/f443b49093cee01bf6c687284299b9d9.

Hibiki, T., Lee, T.H., Lee, J.Y. and Ishii, M., 2006. "Interfacial area concentration in boiling bubbly flow systems". *Chemical Engineering Science*, Vol. 61, No. 24, pp. 7979–7990. ISSN 0009-2509. doi:http://dx.doi.org/10.1016/j.ces.2006.09.009. URL http://www.sciencedirect.com/science/article/pii/S0009250906005847.

Hinze, J.O., 1955. "Fundamentals of the hydrodynamic mechanism of splitting in dispersion processes". *AIChE Journal*, Vol. 1, No. 3, pp. 289–295.

Ishii, M., 1977. "One-dimensional drift-flux model and constitutive equations for relative motion between phases in various two-phase flow regimes". Technical report, Argonne National Lab., Illinois.

Ishii, M. and Hibiki, T., 2006. *Thermo-Fluid Dynamics of Two-Phase Flow*. Springer, New York.

Kataoka, I. and Serizawa, A., 1990. "Interfacial area concentration in bubbly flow". *Nuclear Engineering and Design*, Vol. 120, No. 2-3, pp. 163–180. ISSN 0029-5493. doi:http://dx.doi.org/10.1016/0029-5493(90)90370-D. URL http://www.sciencedirect.com/science/article/pii/002954939090370D.

Lima, L.E.M., 2011. *Análise do modelo de mistura aplicado em escoamentos isotérmicos gás-líquido*. Ph.D. thesis, Faculdade de Engenharia Mecânica, Universidade Estadual de Campinas, Campinas. URL `http://repositorio.unicamp.br/jspui/handle/REPOSIP/264105`.

Nicklin, D.J., 1962. "Two-phase bubble flow". *Chemical Engineering Science*, Vol. 17, No. 9, pp. 693–702. ISSN 0009-2509. doi:http://dx.doi.org/10.1016/0009-2509(62)85027-1. URL `http://www.sciencedirect.com/science/article/pii/0009250962850271`.

Press, W.H., Teukolsky, S.A., Vetterling, W.T., Flannery, B.P. and Metcalf, M., 1996. *Numerical recipes in Fortran 90: the art of scientific computing*, Vol. 2. Cambridge University Press, 1st edition.

Sekoguchi, K., Fukui, H., Matusoka, T. and Nishikawa, K., 1974. "Studies on statistical characteristics of bubbles by electrical resistivity probe, i, ii". *trans. JSME*, Vol. 40, pp. 2295–2310.

Shoham, O., 2006. *Mechanistic modeling of gas-liquid two-phase flow in pipes*. Society of Petroleum Engineers, Richardson, Texas.

Taitel, Y., Barnea, D. and Dukler, A.E., 1980. "Modelling flow pattern transitions for steady upward gas-liquid flow in vertical tubes". *AIChE Journal*, Vol. 26, No. 3, pp. 345–354. ISSN 0001-1541.

Taitel, Y. and Dukler, A.E., 1976. "A model for predicting flow regime transitions in horizontal and near horizontal gas-liquid flow". *AIChE Journal*, Vol. 22, No. 1, pp. 47–55.

Zuber, N. and Findlay, J.A., 1965. "Average volumetric concentration in two-phase flow systems". *Journal of Heat Transfer*, Vol. 87, No. 4, pp. 453–468.

8. RESPONSIBILITY NOTICE

The authors are the only ones responsible for the printed material included in this paper.